JOURNAL OF APPLIED ELECTROCHEMISTRY 26 (1996) 90–94

Physico-chemical properties of Zn–Fe alloy deposits from an alkaline sulphate bath containing triethanolamine

V. NARASIMHAMURTHY, B. S. SHESHADRI*

Department of Studies in Chemistry, Central College, Bangalore University, Bangalore 560 001, India

Received 2 March 1995; revised 28 July 1995

The composition, properties, structure and morphology of Zn–Fe alloy deposits obtained from an alkaline sulphate bath have been investigated. The bath containing triethanolamine produced smooth, uniform and bright Zn–Fe alloy deposits having the desired 15–25% Fe. The deposition potentials of Zn–Fe alloy lie between the potentials of the individual metals. Increased current density lowered the Fe percentage in the alloy deposit. The structure and morphology of the alloy deposits were found to depend on the Fe percentage in the alloy.

1. Introduction

Electrodeposited zinc alloys find extensive use as a viable substitute for zinc and cadmium metals in the corrosion protection of steel [1–4]. Recently electrodeposited Zn–Fe alloy containing 15–25% Fe showed excellent corrosion resistance, weldability, workability, formability and good paintability. Alloys of Zn–Fe are electrodeposited from acid sulphate [5, 6], chloride and sulphate-chloride baths [7].

The alkaline Zn–Fe alloys system is very similar to the noncyanide alkaline zinc system [8]. Sree and Ramachar [9] were the first to report an alkaline pyrophosphate bath for electrodeposition of Zn–Fe alloy. The disadvantages of using toxic cyanide and ammonia containing alkaline sulphate baths are loss of ammonia at high operating temperature, problems in maintaining the deposition process and effluents from the cyanide bath. A literature survey also indicated that no attempt has been made to replace ammonia. Ethanolamines seem to be logical substitute for ammonia and the use of ethanolamine has been shown to improve the quality deposit and also to stabilize the bath [10, 11]. Earlier investigations [12, 13] showed that triethanolamine (TEA) can be effectively used as a complexing agent in acid and alkaline sulphate baths for obtaining smooth and uniform Zn–Fe alloy containing 15–25% Fe. The present work reports results on the study of composition, properties, structure and surface morphology of electrodeposited Zn–Fe alloy deposits obtained from an alkaline sulphate bath containing TEA.

2. Experimental procedure

The plating bath solutions were prepared using distilled water and laboratory grade chemicals. The bath solution was purified as described elsewhere [14]. The optimum bath composition is given in Table 1. Electrodeposition was carried out galvanostatically at 323 K under stirred conditions. A stainless steel anode was used. To determine the composition of the alloy deposits, the deposited alloy was dissolved in 20% HNO_3 and analysed for metal content by atomic absorption spectrometry.

Deposition potentials are referred to the saturated calomel electrode using a scanning potentiostat.

The alloy samples were heat treated in an evacuated glass tube (pressure 10^{-6} torr) in a furnace at 633 K for 30 min. After heating the glass tube was removed from the furnace and allowed to cool to room temperature. It was then broken open and the samples were removed and used.

The adhesion of Zn–Fe alloy deposits on the base metal was tested by a standard bending test. The porosity of alloy deposit was determined by the ferroxyl test. The microhardness of the alloy deposits was determined on the Vickers scale. The ductility of the deposits was evaluated by a bending test method. The tensile strength of the deposits was determined using a tensile testing machine (Tensiometer).

The phase structures of the Zn–Fe alloy deposits were determined by X-ray powder diffraction (filter CuK_α, 30 kV, 20 mA, 4000 counts). Zn–Fe alloys were deposited to 30 μm on a copper plate for X-ray analysis.

Scanning electron microscopy was used to study the surface morphology of the deposits coated over a polished copper substrate.

3. Results and discussions

3.1. *Composition*

Figure 1 shows the cathodic polarization curves for the alloy deposition on copper cathode (curve (a)).

* Author to whom correspondence should be sent.

0021-891X/93

Table 1. Bath composition and operating conditions for electrodeposition of Zn–Fe alloy

Component	*Range studied*	*Optimum*
Total metal content	0.1–0.4 M	0.1 M
$ZnSO_4 \cdot 7H_2O$	0.05–0.09 M	0.09 M
$FeSO_4 \cdot 6H_2O$	0.01–0.05 M	0.01 M
Ascorbic acid	0.005–0.1 M	0.01 M
Triethanolamine	0.00625–1.6 M	0.1 M
Na_2SO_4	10–60 g dm^{-3}	30 g dm^{-3}
NaOH	40–160 g dm^{-3}	80 g dm^{-3}
pH	–	> 14
Temperature	293–353 K	323 K
Current density	2–80 A dm^{-2}	10 A dm^{-2}
Agitation	–	normal

The figure also shows the polarization characteristics of the deposition of individual metals (curves (a) and (b)). The deposition potential of iron was about −0.71 V, whereas for zinc it is −0.93 V. The deposition potential of alloy lies between that of iron and zinc (−0.82 V). This value is less negative than the deposition potential of zinc and more negative to iron indicating the alloy deposition to be of the regular codeposition type [15].

To study the effect of metal ion ratio in the bath on the alloy composition, the bath zinc to iron ratio was varied from 50 : 50 to 90 : 10. Figure 2 shows the variation of alloy composition with bath composition obtained at three different current densities (5, 10 and 40 A dm^{-2}). A bath solution containing 60% Fe produced an alloy deposit with 69% Fe indicating that the more noble iron deposited preferentially, leading to regular co-deposition. At higher current densities (> 40 A dm^{-2}), the percentage of iron coincided with the composition reference line (CRL) AB. Thus the iron content in the alloy deposit was the same as

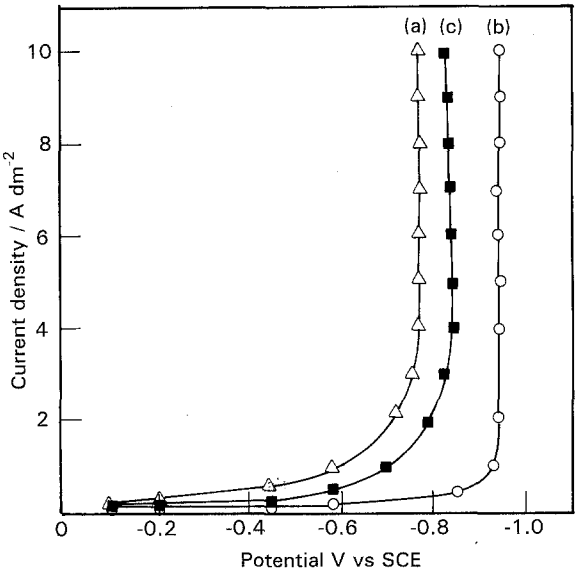

Fig. 1. Cathodic polarization curves for the deposition of Zn–Fe alloy from the alkaline sulphate bath. All solutions contained triethanolamine (0.1 M), ascorbic acid (0.02 M), Na_2SO_4 (30 g dm^{-3}), NaOH (80 g dm^{-3}). Curves: (a) deposition of iron alone; (b) deposition of zinc alone and (c) deposition of Zn–Fe alloy (bath contained same zinc and iron concentrations as those in the individual baths).

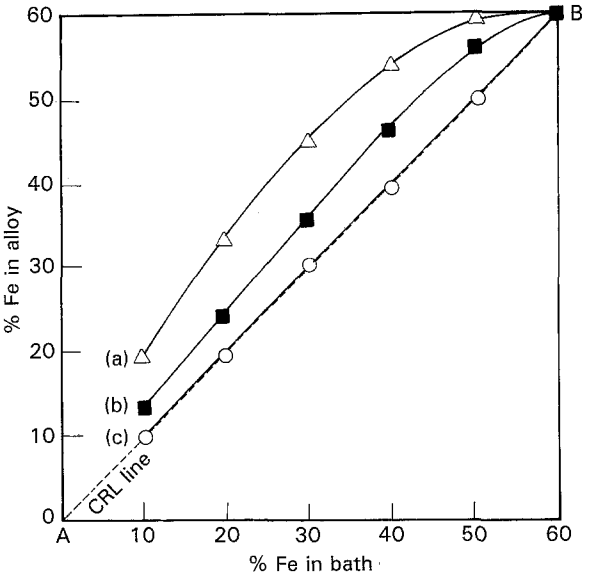

Fig. 2. Effect of zinc to iron ratio in the bath on composition of Zn–Fe alloy. Bath composition: [Zn^{2+}] 0.01–0.09 M; [Fe^{2+}] 0.01–0.05 M; TEA (0.1 M); ascorbic acid (0.02 M); Na_2SO_4 (30 g dm^{-3}); NaOH (80 g dm^{-3}). Thickness 600 nm; temperature 323 K; stirred; pH > 14. Current density: (a) Cd 5, (b) Cd 10 and (c) Cd 40 A dm^{-2}.

that of the iron content in the bath. This clearly indicates that Zn–Fe alloy deposited from the alkaline sulphate bath containing TEA is of the regular codeposition type.

The effect of current density on alloy composition is illustrated in Fig. 3. With gradual increase in current density (up to 20 A dm^{-2}) the Fe percentage in the alloy decreased rapidly. With further increase in current density (20 to 80 A dm^{-2}), the Fe percentage in the alloy deposit attained a steady value, approaching the Fe percentage in the bath. This may be due to the rate at which the metal ion deposition is limited by the

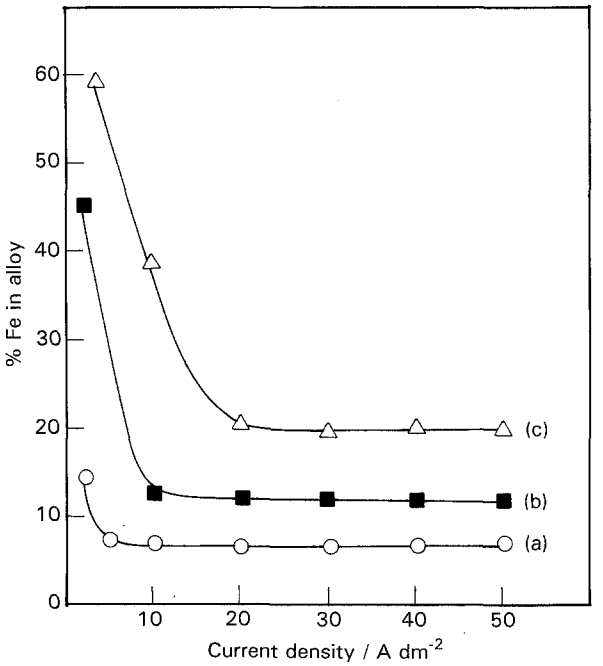

Fig. 3. Effect of current density on composition of Zn–Fe alloy. Bath composition: [Zn^{2+}] 0.09 M; [Fe^{2+}] 0.01 M; TEA (0.1 M); ascorbic acid (0.02 M); Na_2SO_4 (30 g dm^{-3}); NaOH (80 g dm^{-3}). Thickness: 600 nm; temperature: 323 K; pH > 14; stirred. Temperature: (a) 298, (b) 323 and (c) 353 K.

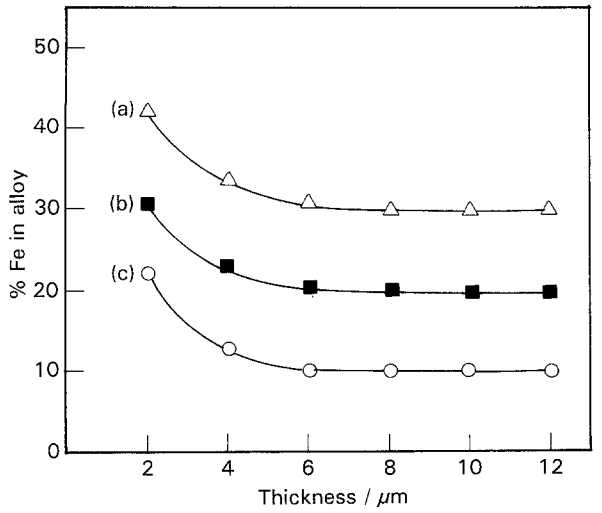

Fig. 4. Effect of thickness on composition of Zn–Fe alloy. Bath composition: as in Fig. 3. Composition: (a) 70:30 Zn:Fe, (b) 80:20 Zn:Fe and (c) 90:10 Zn:Fe.

rate of mass transfer of metal ions towards the cathode.

Increase in bath temperature increased the Fe percentage in the alloy deposit indicating a diffusion controlled alloy deposition. Increase in Fe percentage in an alloy with bath temperature further confirms that the alloy deposition is of regular codeposition type.

The variation of the alloy composition with thickness is shown in Fig. 4. Increase in thickness produced lower Fe percentage in the deposit which reached an almost constant value at higher thickness.

3.2. *Properties*

The adhesion of the deposits to the base metal was tested by a standard bending test. Zn–Fe alloy samples deposited to different thicknesses (2–12 μm) on steel (1 in × 4 in) were subjected to bending tests. The alloy coatings did not develop any visual cracks even after 180° bending. This shows good adhesion of the alloy deposits to the base metal.

Porosity tests were conducted on Zn–Fe alloy coated on steel panels (3 × 3 inch^2) to a thickness of 2–12 μm. A filter paper soaked in potassium ferricyanide solution (1%) was placed on alloy coated steel panels. Appearance of blue spots on the filter paper with time was observed. The number of blue spots appearing on the filter paper with time is the measure of porosity of the deposit. The alloy deposits were pore free at sufficient thickness (> 6 μm).

Table 2. Effect of temperature on composition of Zn–Fe alloy deposited from an alkaline sulphate bath: $ZnSO_4 \cdot 7H_2O$ 0.09 M, $FeSO_4 \cdot 6H_2O$ 0.01 M, TEA 0.1 M, ascorbic acid 0.02 M, Na_2SO_4 30 g dm^{-3}, NaOH 80 g dm^{-3}, current density 20 A dm^{-2}, pH > 14, Thickness 600 nm, stirred

Temperature/K	*Zn–Fe alloy*/%Fe
303	9.25
323	12.28
353	38.33

Table 3. Effect of Fe percentage on microhardness and tensile strength of Zn–Fe alloy

Fe in alloy /%	*Hardness on Vickers scale* /VHN	*Tensile strength* /N mm^{-2}
0	85.20	62.56
10	126.50	89.47
15	140.61	118.33
20	147.34	122.12
25	155.12	91.68
30	159.54	77.32

Table 4. Rest potentials values vs SCE

Zinc	−1013 mV
Zn–Fe (10% Fe)	−913 mV
Zn–Fe (15% Fe)	−900 mV
Zn–Fe (20% Fe)	−852 mV
Zn–Fe (25% Fe)	−834 mV
Zn–Fe (30% Fe)	−802 mV
Mild steel	−570 mV

Tensile strength measurements were made using specimens machined from Zn–Fe alloy deposits (4 μm thick). The dependency of tensile strength on % Fe in the alloy is given in Table 3. The highest tensile strength value was observed for 20% Fe containing alloy. This may be due to the finer grained deposits at this particular composition.

The ductilities of the deposits were measured by a bending test method. The Zn–Fe alloy deposited to a thickness of 10 μm on steel panels (1 × 4 inch^2) were subjected to bending up to 180°. The alloy deposits did not develop any cracks at the point of bending. This demonstrates that the Zn–Fe alloy deposits have excellent ductility.

The microhardness of 12 μm thick Zn–Fe alloy specimens was measured. The hardness of the alloy deposit increased with increase in % Fe (Table 3).

The rest potentials of Zn and Zn–Fe alloy were measured with reference to SCE in 3.5% NaCl solution. Table 4 shows the values of rest potentials of the alloy which are significantly more positive to zinc and more negative to steel under identical conditions. This shows that Zn–Fe alloy deposits are good sacrificial coatings for corrosion protection of steel.

In another test Zn and Zn–Fe alloy electrodeposited on steel samples (12 μm thick) were immersed in 3% NaCl solution. Rust spots were observed after 40 h in the case of zinc coated steel and after 90 hours for Zn–Fe alloy having 20% Fe coated on the steel.

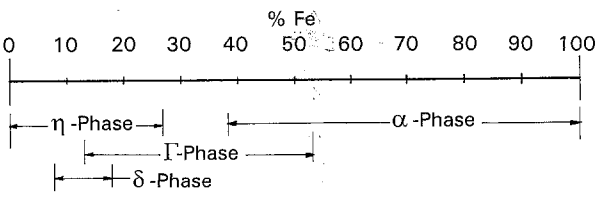

Fig. 5. Relationship between phase and Fe percentage in Zn–Fe alloy electrodeposited from an alkaline sulphate bath containing TEA.

3.3. *Structure and morphology*

The phase structure of electrodeposited Zn–Fe alloy is very complex. However, the phase structure of thermally prepared Zn–Fe alloys have been reported by earlier workers [16–18]. In the present work, the phase structure of electrodeposited Zn–Fe alloy was determined by X-ray powder diffraction.

Figure 5 shows the relationship between the phase and the Fe percentage in the Zn–Fe alloy. Alloy containing low iron content showed intermetallic phases consisting of η, δ and Γ, whereas iron-rich alloy showed predominantly an α phase. This agrees with the observations of earlier workers [19–23]. Thus, electrodeposited Zn–Fe alloy from an alkaline sulphate bath containing triethanolamine produced intermetallic phases which coexist over a wide range of composition. These are: η (9–27% Fe), δ (8–18% Fe), Γ (13–53% Fe) and α (38.5–100% Fe).

The surface morphology of Zn–Fe alloy deposits was examined using scanning electron microscopy (SEM). The morphology of the deposits was found

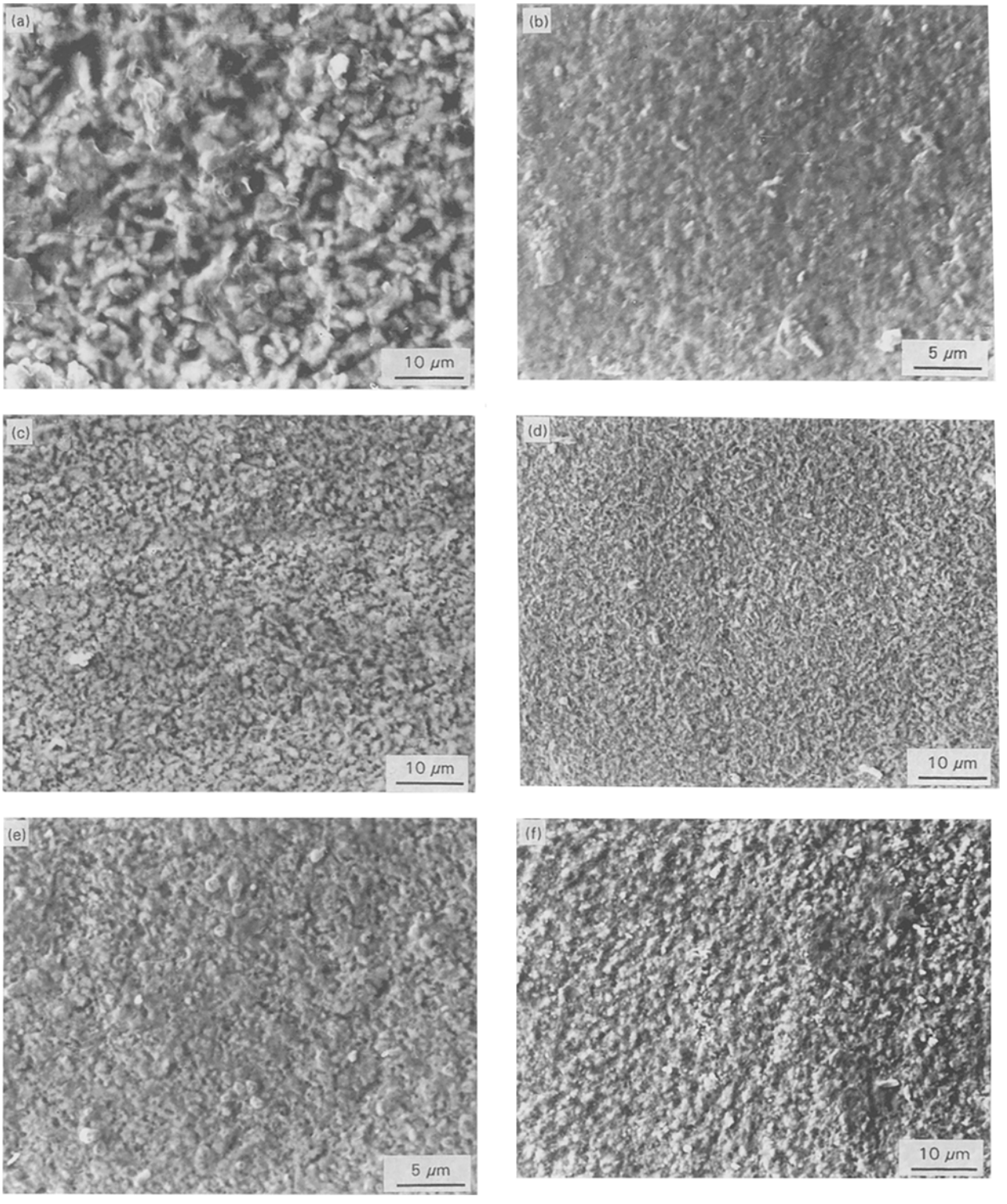

Fig. 6. Scanning electron micrographs of Zn–Fe alloy containing different Fe percentages from an alkaline sulphate bath containing TEA (3500×): (a) 0% Fe, (b) 10% Fe, (c) 15% Fe, (d) 20% Fe, (e) 25% Fe and (f) 30% Fe.

to depend on the Fe percentage in the alloy (Fig. 6). Smooth, uniform and finer grained deposit structure was observed for Zn–Fe alloy containing 20% Fe.

4. Conclusions

Zn–Fe alloy containing 15–25% Fe electrodeposited from an alkaline sulphate bath containing TEA is of regular codeposition type. The alloy deposits obtained were smooth, uniform and fine grained. The cathodic current–potential curve during Zn–Fe alloy deposition was intermediate between those of individual metals. The Fe content in the alloy was more than that of iron in the bath. Increase in temperature of the operating bath increases the Fe content in the alloy. Increase in current density decreases the Fe content in the alloy which reached a steady value. Increase in the thickness of the alloy leads to a constant alloy composition. Intermediate phases appeared in electrodeposited Zn–Fe alloy. Smooth, uniform and fine grained deposits were observed morphologically for Zn–Fe alloy containing 20% Fe.

Acknowledgement

The authors are thankful to the Director of the Geological Survey of India for atomic absorption facilities and the Chairman, MRC, I.I.Sc., Bangalore for SEM data. One of the authors (V.N.) is grateful to C.S.I.R., New Delhi for the award of Senior Research Fellowship.

References

[1] G. G. Kraft, *Metal Finish.* **88** (1990) 29.
[2] R. Winand, *Surf. Coat. Tech.* **37** (1989) 65.
[3] B. Knotkova, E. Boubelova and J. Mechaura, *Koroze. Ochr. Mater.* **27** (1983) 25.
[4] L. Nanova, V. Kozhukharov and Velinov, *Galvanotechnik* **76** (1985) 453.
[5] T. Adaniya, T. Hara, M. Sagiyama, T. Homa and T. Watanable, *Plat. Surf. Finish.* **72** (1985) 52.
[6] F. W. Salt, *Electroplating & Metal Finish.* **9** (1956) 3.
[7] F. Jepson, S. Meecham and F. W. Salt, *Trans. IMF* **32** (1955) 160.
[8] T. Tsuchida and I. Suzuki, *US Patent 4 581 110* (1986).
[9] V. Sree and T. L. Ramachar. *J. Sci. Industr. Res.* **15B** (1958) 439.
[10] Y. N. Shalimov *et al.*, *Zasch. Met.* **13** (1977) 623.
[11] A. I. Falicheva and B. A. Speridonov, *ibid.* **12** (1976) 342.
[12] V. Narasimhamurthy and B. S. Sheshadri, *Plat. Surf. Finish.*, accepted.
[13] V. Narasimhamurthy and B. S. Sheshadri, *Metal Finish.* submitted.
[14] S. Sankarapapavinasam, F. Pushpanadan and M. F. Ahmed, *Metal Finish.* **87** (1989) 9.
[15] A. Brenner, 'Electrodeposition of Alloys', Vol. 1, Academic Press, New York and London (1963) p. 343.
[16] E. J. Raub and K. Muller, 'Fundamentals of Metal Deposition', Elsevier, New York (1967).
[17] O. Kubaschewkki, 'Iron-Binary Phase Diagrams', Springer-Verlag, Berlin (1982) p. 173.
[18] M. Hausen, 'Constitution of Binary Alloys', McGraw-Hill, New York, Toronto, London (1958) p. 737.
[19] K. Kondo, S. Hinotani, Y. Ohmori, *J. Appl. Electrochem.* **18** (1988) 154.
[20] M. Gu and A. R. Marder, *Plat. Surf. Finish.* **78** (1991) 77.
[21] L. A. Giannuzzi, A. S. Ramani, P. R. Howell, H. W. Pickering and W. R. Bitler, *ibid.* **80** (1993) 54.
[22] Y. Shima, S. Terasaka, K. Nakawaka, T. Hara and T. Honma, *Testue-to-Hagaue* **8** (1986) 956.
[23] M. Kimoto, S. Wakano and A. Shibuya, *ibid.* **8** (1986) 961.